Song, Shuguang, **Niu, Yaoling**, Zhang, Guibin & Zhang, Lifei (2018). Two epochs of eclogite metamorphism link 'cold' oceanic subduction and 'hot' continental subduction, the North Qaidam UHP belt, NW China. *Geological Society, London, Special Publications* **474**: 1-15. https://doi.org/10.1144/SP474.2

Paper in:

ZHANG, L.F., ZHANG, Z., SCHERTL, H.-P. & WEI, C. (eds) HP–UHP Metamorphism and Tectonic Evolution of Orogenic Belts. ***Geological Society, London, Special Publications, 474,*** https://doi.org/10.1144/SP474.2

Two epochs of eclogite metamorphism linking "cold" oceanic subduction and "hot" continental subduction, the North Qaidam UHP belt, NW China

Shuguang Song[1], Yaoling Niu[2,3], Guibing Zhang[1], Lifei Zhang[1]

1. *MOE Key Laboratory of Orogenic Belts and Crustal Evolution, School of Earth and Space Sciences, Peking University, Beijing 100871, China*

2. *Department of Earth Sciences, Durham University, Durham DH1 3LE, UK*

3. *Institute of Oceanology, Chinese Academy of Science, Qingdao 266071, China*

Abstract.

Eclogites in the HP and UHP belts record subduction zone processes. Our current understanding of subduction-zone processes largely comes from petrological and geochemical studies of exhumed eclogites and eclogitic rocks. While the mechanisms of exhumation remain poorly understood, exhumed eclogites of seafloor protoliths record low temperature (mostly < 600 °C), high pressure and "wet" environments, i.e., relatively "cold" subduction with highly hydrous minerals such as lawsonite. On the other hand, exhumed eclogites of continental crustal protoliths record relatively "hot" (T > 650 °C) and "dry" UHPM conditions. Here we investigate some eclogites from two ophiolite sequences that intercalated in the North Qaidam UHPM belt, which is genetically associated with continental subduction/collision. The observations of lawsonite-pseudomorphs in garnets, garnet compositional zoning, mineral and fluid inclusions in zircons, and zircons with distinct trace element patterns and U-Pb ages all suggest that these eclogites represent two exhumation episodes of subduction-zone metamorphic rocks: the early “cold” and “wet” lawsonite-eclogite and the late “hot” and “dry” UHP kyanite-eclogite. The early lawsonite-bearing eclogite give metamorphic ages of 470-445 Ma and the later kysnite-bearing eclogite gives metamorphic ages of 438-420 Ma, with a time gap of ~ 7-10 Myrs. This gap may represent the timescale for transition from oceanic subduction and continental subduction to depths greater than 100 km. We conclude that evolution from oceanic subduction to continental collision and subduction was a continuous process.

Keywords: Two episodes of eclogite metamorphism, “cold and wet” oceanic subduction, “hot and dry” continental subduction, North Qaidam UHPM belt

Introduction

Eclogite, as an important rock type within orogenic belts, records processes of subduction and exhumation of both oceanic and continental lithospheric materials. They usually occur in two individual end-member subduction zones, i.e., the oceanic-type and continental-type, within the continental orogenic belts.

Oceanic subduction and continental subduction zones are distinctive in rock assemblage and their detailed dynamics of subduction processes are only poorly known

(Ernst, 2001; Maruyama et al., 1996; Song et al., 2006; 2014a; Rubatto et al., 2011). Relationship between the oceanic subduction (usually cold and negative buoyancy) and continental subduction (usually hot and buoyancy) is also an issue of ambiguity. As to be a consensus, continental crust is less dense than that of the oceanic counterpart, and less likely to sink into the mantle (e.g. Brueckner, 2011). Therefore, a pull force from previously subducted oceanic lithosphere plays an important role in dragging the continental lithosphere to the depths greater than 100 km (e.g., Chemenda et al., 1996; Ernst, 2005; Brueckner, 2006).

Most high-pressure and ultrahigh-pressure metamorphic zones record complex process of subduction and exhumation, for example, two cycles of yo-yo subduction and exhumation would occur within less than 20 Myr (Robbuto et al., 2011), and two orogenic cycles were recorded in one eclogite sample (Herwartz et al., 2011). Transition from oceanic subduction to continental collision and subduction, on the other hand, is a more complex process and two aspects remain to be particularly figured out: (1) the influence upon the former subducted oceanic slab during the continental collision/subduction, and (2) the timescale for the transition from oceanic subduction to continental subduction and exhumation. Presence of UHP metamorphic ophiolite sequences within the continental subduction zones (e.g., Zhang et al., 2008; Song et al., 2006, 2009) provide opportunities to reveal the two cycles of eclogite-facies metamorphism and transition of oceanic-continental subduction.

In this paper, we report two epochs of eclogite-facies metamorphism that recorded early lawsonite-eclogite to late kyanite-eclogite in some individual samples from the

North Qaidam UHP metamorphic belt, which confirm a complete process from "cold" oceanic subduction to "hot" continental subduction. This process will help us in understanding dynamic process of connection between the oceanic subduction and the subsequent continental subductions.

Mineral abbreviations are after Whitney and Evans (2010).

Geological Setting

Two kinds of subduction belts, i.e., the North Qilian oceanic "cold" subduction zone in the north and the North Qaidam continental subduction belt in the south, extend parallel in the northern Qinghai-Tibet Plateau. The North Qilian orogenic belt in the north is the type oceanic suture zone and contains early Paleozoic ophiolite sequences, HP metamorphic belts, island-arc volcanic rocks and granitic plutons, Silurian flysch formations, Devonian molasse, and Carboniferous to Triassic sedimentary cover sequences (see Song et al., 2013 and reference therein). Lawsonite in eclogite and Mg-carpholite in metapelite provide convincing evidence that the North Qilian HP metamorphic belt records cold oceanic lithosphere a low geothermal gradient (6–7 °C/km) in the early Paleozoic (Zhang et al., 2007; Song et al., 2007).

The North Qaidam UHPM belt in the south is located in the north margin of the Qaidam Basin, between the Qilian Block and Qaidam Block, and extends for about 400 km (see Fig. 1). The North Qaidam UHPM belt mainly consists of granitic and pelitic gneisses intercalated with blocks of eclogite and varying amounts of ultramafic rocks, especially garnet peridotite. The rock assemblages suggest that this belt is typical of a continental-type subduction zone (Song et al., 2014a and references therein), different from the "cold", oceanic-type subduction of the North Qilian suture zone.

Coesite inclusions have been identified in zircon and garnet from metapelite and eclogite at Dulan, Xitieshan and Yuka (Yang et al., 2002; Song et al., 2003a,b, 2006; Zhang G. et al., 2009; Zhang et al., 2010; Liu et al., 2012) and diamond in zircon from the garnet peridotite at Lüliangshan (Song et al., 2005), respectively. P-T estimates of the enclosing eclogite and garnet peridotite establish the North Qaidam eclogite belt as an Early Paleozoic UHPM terrane exhumed from depths of 100−200 km.

Two rock-types of eclogitic protoliths have been identified in the North Qaidam UHPM belt: (1) the 850-820 Ma CFBs with mantle-plume origin (Chen et al., 2009; Song et al., 2010; Zhang et al., 2010) and (2) 540-500 Ma ophiolite with UHP metamorphic harzburgite, cumulate gabbro (kyanite eclogite) and N- to E-type basalts (Song et al., 2006, 2009; Zhang, 2008).

Sample Petrography

Two types of eclogite samples from two sections in the well-studied Dulan UHP terrane were carefully investigated (see localities in Fig. 1a). One is the bimineral eclogites with protoliths of low-K tholeiitic basalt (Song et al., 2006), the other is kyanite eclogite from cumulate gabbro in a UHP metamorphic ophiolite sequence (e.g. Zhang et al., 2008).

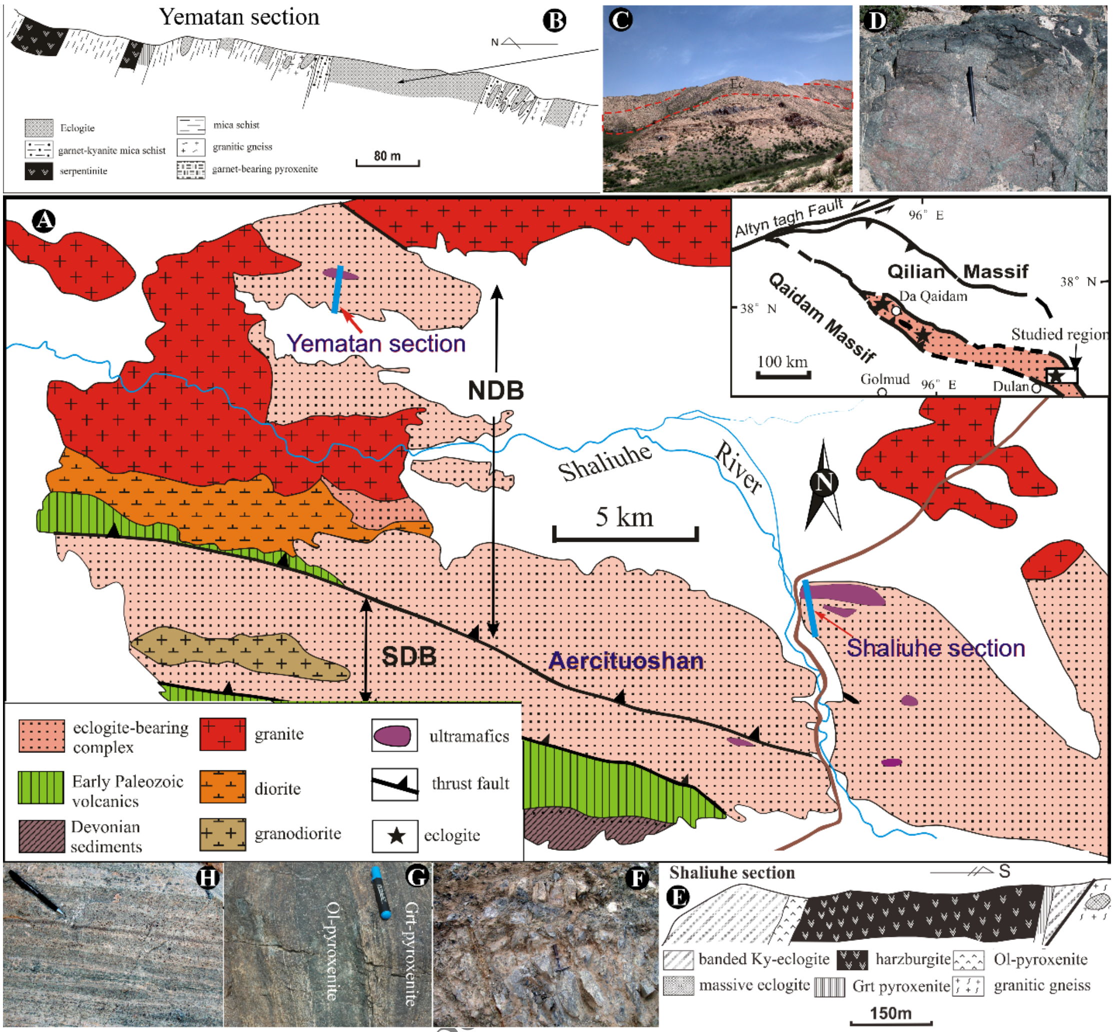

Fig. 1. (A) Geological map of the Dulan UHPM terrane with two ophiolitic sections. The Yematian section (B) consists of UHP metamorphosed serpentinite, garnet pyroxenite, gabbroic and basaltic eclogites (C, D). The Shaliuhe section (E) consists of UHP metamorphosed harzburgite (F), garnet pyroxenite and olivine pyroxenite (G), kyanite-eclogite (cumulate gabbro) (H).

Basaltic bimineral eclogite in the Yematan section

Samples was collected from a large massive eclogite block (200×800 m in size) in the Yematan section; this cross-section exposes blocks of garnet-bearing, strongly garnet-bearing serpentinized peridotite (Mattinson et al., 2006), garnet-bearing pyroxenite and eclogite intercalated with coesite bearing metapelite (Yang et al., 2002; Song et al., 2003, 2006, 2009) and 910-950 Ma granitic gneisses (Song et al., 2012) (Fig. 1b). The garnet pyroxenite was interpreted to be an ultramafic cumulate and the eclogite blocks are geochemically similar to present-day N-type to E-type MORB (Song et al, 2003b, 2006). This rock assemblage resembles a dismembered ophiolite (Song et al., 2009) with protolith ages of ~ 500 Ma (Han, 2015).

The studied eclogite samples (2D73, 2D155 and 11YM29) are a very fresh, show a granoblastic texture without being deformed, and consist of garnet (~35 %), omphacite (~60 %), rutile (~1-2%) with very rare phengite and the least amphibole overprinting (Fig. 2a). The protolith is low-K basalt in composition and exhibits geochemical characters of N-MORB affinity (Song et al., 2006). We name it basaltic eclogite. In this eclogite, omphacite is equigranular, relatively small in size and chemically homogeneous; garnet occurs as porphyroblasts uniformly distributed in the matrix of omphacite (Fig. 2a).

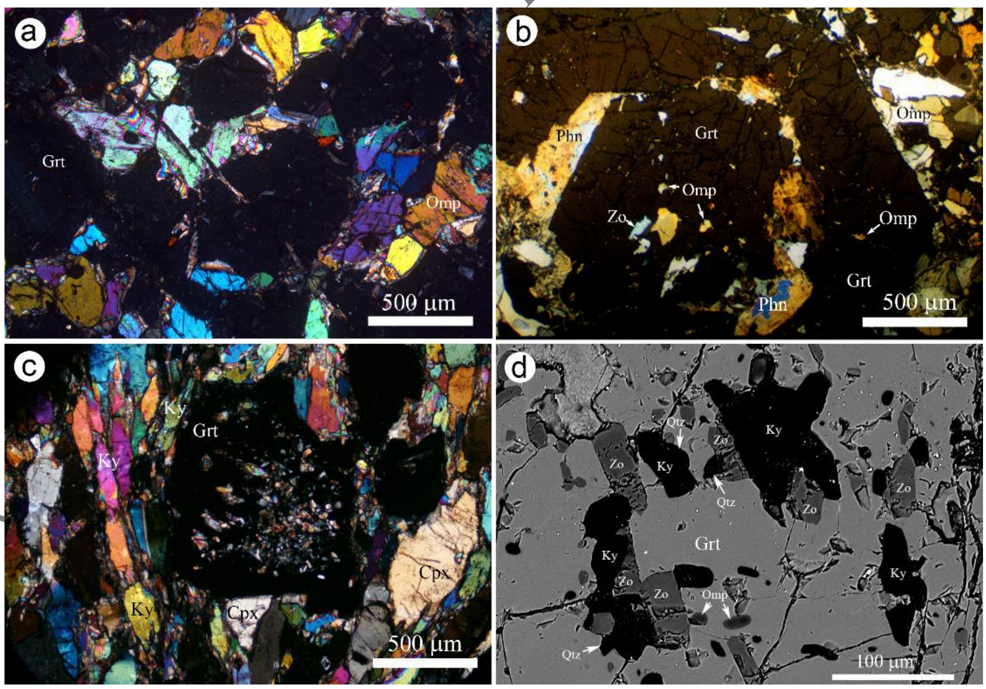

Fig. 2. Photomicrographs showing textures of the two types of eclogites. (a) granoblastic texture of the basaltic bimineral eclogite (2D73) in the Yematan section. (b) Garnet (Grt) porphyroblast show two stages of growth. (c) Ky-eclogite (4C05) with mineral assemblage Grt + Omp + Ky + Rt. Garnet has a large quantity of mineral inclusions in the core domain. (d) Mineral inclusions kyanite (Ky), zoisite (Zo), omphacite (Omp) and quartz (Qtz) in garnet. The assemblage Ky + Zo + Qtz is most

likely the product of lawsonite decomposition.

Gabbroic kyanite-eclogite in Shaliuhe ophiolite sequence

The kyanite eclogite (including samples KL61, 4C05, 4C19) that was collected from the well-studied Shaliuhe UHPM ophiolite section, which contains (1) serpentinized harzburgite, (2) garnet-bearing pyroxenite and olivine pyroxenite, (3) kyanite-eclogite, and (4) massive eclogite (Fig. 1 E-H). The peridotite block is dark-colored, strongly serpentinized and is apparently conformable with pyroxenites and kyanite-eclogite. Relic olivine, opx with two types of olivine (relic olivine from the oceanic mantle and metamorphic olivine during UHP metamoephism) (Zhang et al., 2008; Song et al., 2009). Both the garnet-bearing pyroxenite and kyanite-eclogite retain a banded structure that has been confirmed as inherited from original ultramafic and gabbroic cumulates (Fig. 1, G and H). Geochemical analyses further indicate that this banded kyanite-eclogite has characteristics of cumulate gabbro by high contents of Al2O3 (17.2–22.7 wt%), CaO (12.5–13.5 wt%), MgO (7.2–13.5 wt%), Cr (422–790 ppm), Ni, Sr, low TiO2 and REE, and show strong positive Eu anomalies (Eu* 1.51–2.08) (Zhang et al., 2008). We therefore name it gabbroic Ky-eclogite.

The Ky-eclogite has the mineral assemblage of Grt, Omp, Ky and Rt with retrograde overprinting by amphibole. Phengite is a minor phase that occasionally occurs in matrix or as inclusion in Omp and garnet, and no Ep or Zo was found in the matrix. Grt-Omp-Phn-Ky geothermoborameter of Ravna and Terry (2004) yielded peak P-T conditions of P = 2.7-3.4 GPa and T = 630-770 °C (Song et al., 2003; Zhang et al., 2008).

Two epochs of eclogite metamorphism recorded in garnet

All garnet porphyroblasts in the gabbroic and basaltic eclogite samples (2D73) show clear core-rim structure; they are defined by both mineral inclusions and chemical patterns and exhibit clear two-stage overgrowth (Fig. 2b). In the kyanite eclogite (KL61), the core domain of garnet contains abundant mineral inclusions, but the rim domain is fairly clean (Fig. 2c). This core-rim structure is a common feature for garnet in all low-temperature (especially lawsonite-bearing) eclogites (e.g. Clarke et al., 1997; Song et al., 2007), but less common in the high-temperature eclogites in the continental-type UHPM belt.

Lawsonite pseudomorph in garnet from the Ky-eclogite

Mineral inclusions in the core domain of garnets from the Ky-eclogite are kyanite, zoisite, omphacite and quartz. They show rectangular and triangular shapes (Fig. 2d). Zoisite inclusions are characterized by extremely low FeOt in composition [Ps = $100*Fe^{3+}/(Fe^{3+}+Al)$ = 0.1-2.1 mol%] (Table 1). This mineral assemblage comprises lawsonite psedomorphs and define a possible reaction of the form:

$4CaAl_2 [Si_2O_7](OH)_2(H_2O) = 2Ca_2Al_3(Si_2O_7)(SiO_4)O(OH) + Al_2SiO_5 + SiO_2 + 7H_2O$ (i.e., Lws = Zo + Ky + Qtz + H_2O).

Omp inclusions in garnet have slightly higher mole aegrine (Ae = 6.1-7.0 mol%) and lower jadeite (Jd = 25-27 mol%) than Omp in the matrix (Ae = 0, Jd =35-39 mole%; Table 1), suggesting a lower temperature condition in the core domain.

The numerous lawsonite pseudomorphs in garnet suggest that lawsonite was ubiquitous during the first epoch of lawsonite-eclogite facies metamorphism associated with cold and water-saturated oceanic subduction.

Garnet compositional profiles

Garnet from the gabboic Ky-eclogite have much higher MgO and CaO than from the basaltic eclogite. A porphyroblast garnet from the gabbroic eclogite was chosen for compositional profile analyses. As shown in Figure 3a, two epochs of progressive growth zonation are recognized in the profile; in the core domain, grossular decreases smoothly from center (Grs 23.33 mol%) to core-rim boundary (Grs 21.1 mol%), almandine from 35.65 to 34.91, whereas pyrope increases from 40.37 to 43.01 mol %. Chemical zoning sharply changes in the core-rim boundary; grossular bounds up to 23.87 mol %, almandine to 36.94 mol %, and pyrope drops down to 39.3 mol %.

Some garnet porphyroblasts in sample 2D73 also exhibit core-rim structure; zoisite, amphibole and omphacite occur in the core and phengite inclusions occur at the core-rim boundary (Fig. 2b). Compositional zoning shows similar pattern with sharp change at the core-rim boundary (Fig. 3b).

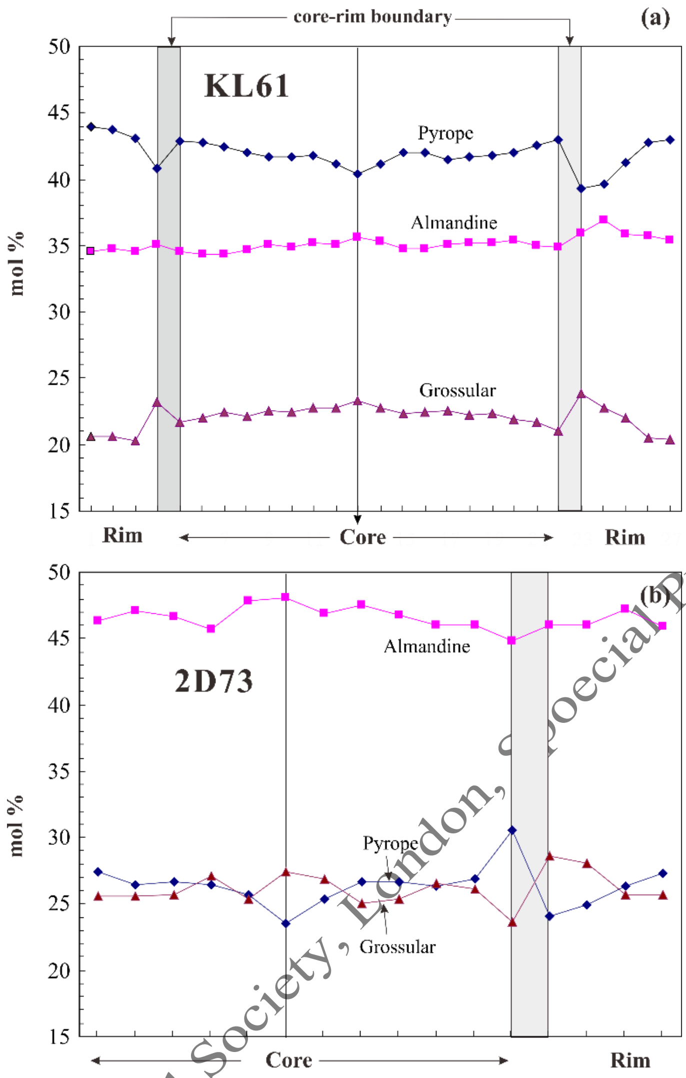

Fig. 3. Composition profiles of garnets from a kyanite-eclogite (KL61) and bimineral eclogite 2D73.

The sharp increase of glossular at the core-rim boundaries can be explained by decomposition of lawsonite with increase of pressure and temperature, which can release large amount of glossular composition into garnet at UHP conditions beyond the lawsonite stability field. Dehydration of lawsonite during continental subduction will give rise to exhumation and decompression melting of the subducted oceanic slab (Song et al., 2014b).

P-T estimate for the Ky-eclogite

Petrographic observations indicate that eclogite-facies metamorphic epoch recorded in the core domain of garnet contains low-tempreture assemblage grt + Omp + Lws +/- Phn + Qtz/Coe + Rt, as lawsonite presents as psudomorphs of Ky + Zo + Qtz. Using compositions of Cpx inclusions in garnet and the garnet around, and assuming presence of Phn, and using the garnet–clinopyroxene Fe^{2+}–Mg exchange thermometer of Ravna (2000) and the geothermobarometry of (Ravna & Terry, 2004), we obtained P-T conditions for the first epoch of eclogite metamorphism at T = 547-603°C and P = 2.6-2.7 GPa, which are well within the lawsonite stability field.

Using the rim composition of garnet and Omp in the matrix, the assemblage Grt + Omp + Ky + Phn in the matrix gave P = 3.2-3.3 GPa and T = 698-721 °C, while Fe^{3+} in omphacite was assumed Fe^{3+} = (Na-Al-Cr).

Two epochs of eclogite metamorphism recorded by zircons

Zircons from six represented, well studied eclogite samples are re-examined for inner structures (CL), mineral inclusions and ages, and zircon REE patterns. These samples include basaltic bimineral eclogite from Yematian ophiolite section (2D73, 2D155, 11YM29), and Ky-eclogite and Grt-pyroxenite from Shaliuhe ophiolite section (4C05, 4C19, 5S23), respectively (Table 2).

Zircon grains from the Shaliuhe gabbroic Ky-eclogite (5S23, Zhang et al., 2008; 2D19, 4C04) and Yematan basaltic eclogite were studied for their Cathodoluminescent (CL) images, mineral inclusions and U-Pb isotopic dating. CL was carried out at The internal zoning was examined using a CL spectrometer (Garton Mono CL3+) equipped on a Quanta 200F ESEM with 2-min scanning time at conditions of 15 kV and 120 nA at Peking University. Zircons were analyzed for U, Pb and Th isotopes using SHRIMP II at Beijing SHRIMP Centre, Chinese Academy of Geosciences. Instrumental conditions and measurement procedures follow Compston et al. (1992). The spot size of the ion beam was about 25 μm in diameter, and the data were collected in sets of five scans through the masses with 2 nA primary $O2^-$ beams. The reference zircon was analyzed first and again after every three unknowns. The measured $^{206}Pb/^{238}U$ ratios in the samples were corrected using reference zircon standard SL13 from a pegmatite from Sri Lanka ($^{206}Pb/^{238}U$=0.0928; 572 Ma) and zircon standard TEMORA (417 Ma) from Australia (Black et al., 2003). The common-Pb correction used the $^{206}Pb/^{204}Pb$ ratio and assumed a two-stage evolution model (Stacey and Kramers, 1975). Concordia ages and diagrams were obtained using Isoplot/Ex (3.0) and the mean ages are weighted means at 95% confidence levels (Ludwig, 2003). Analysis for trace elements of zircons were conducted on Laser-ICP-MS at Chinese University of Geoscience and Peking University. Detailed analytical procedures are similar to those described by Song et al. (2010). The diameter of the laser spot size was 32 μm. Calibrations for elemental concentration were carried out using NIST 610 glass as an external standard, with recommended values taken from Pearce et al. (1997) and using ^{29}Si (for zircon) and ^{49}Ti (for rutile) as an internal standard. NIST 612 and 614 serving as monitoring standards at the same time.

Evidence of zircon structure and mineral/fluid inclusions

All three eclogite samples (2D73, 2D155, 11YM29) from the Yematan ophiolitic sections are all fresh with the least retrograde mineral (Amp) overprinting (Fig. 2a,b).

However, almost all zircons from these samples exhibit core-rim structure in CL images; the core-domains show dark luminescence emission (fluid-rich and high U, Th contents) and fir-tree sector zones, and the rim shows intermediate luminescence emission (Fig. 4). Besides Grt, Omp, Rt inclusions, Qtz and large quantity of water-dominant fluid inclusions are also identified using Raman spectrum in the core domain (Fig. 4a,b), which suggest that the zircon cores were crystallized in a water-rich and quartz-stability condition. As shown in Figure 4c, eclogite-facies mineral inclusions Grt, Omp and Rt are found in both core and rim domains.

CL images suggest that zircons from the gabbroic Ky-eclogite also have two distinct stages of growth with core-rim structure. In sample 5S23, some grains retain magmatic core with oscillatory zones, representing relics from its protolith of cumulate gabbro and therefore having determined the forming age of the ophiolite at 517 ± 11 Ma (Zhang et al., 2008). The textually old core show the dark luminescence emission and weak zoning. The texturally young zircon rim show strong/intimidate luminescence (Fig. 4 c,d), occurs either as rims around old core or as single crystals. Mineral inclusions garnet, omp, rutile are also observed in both core and rim domains.

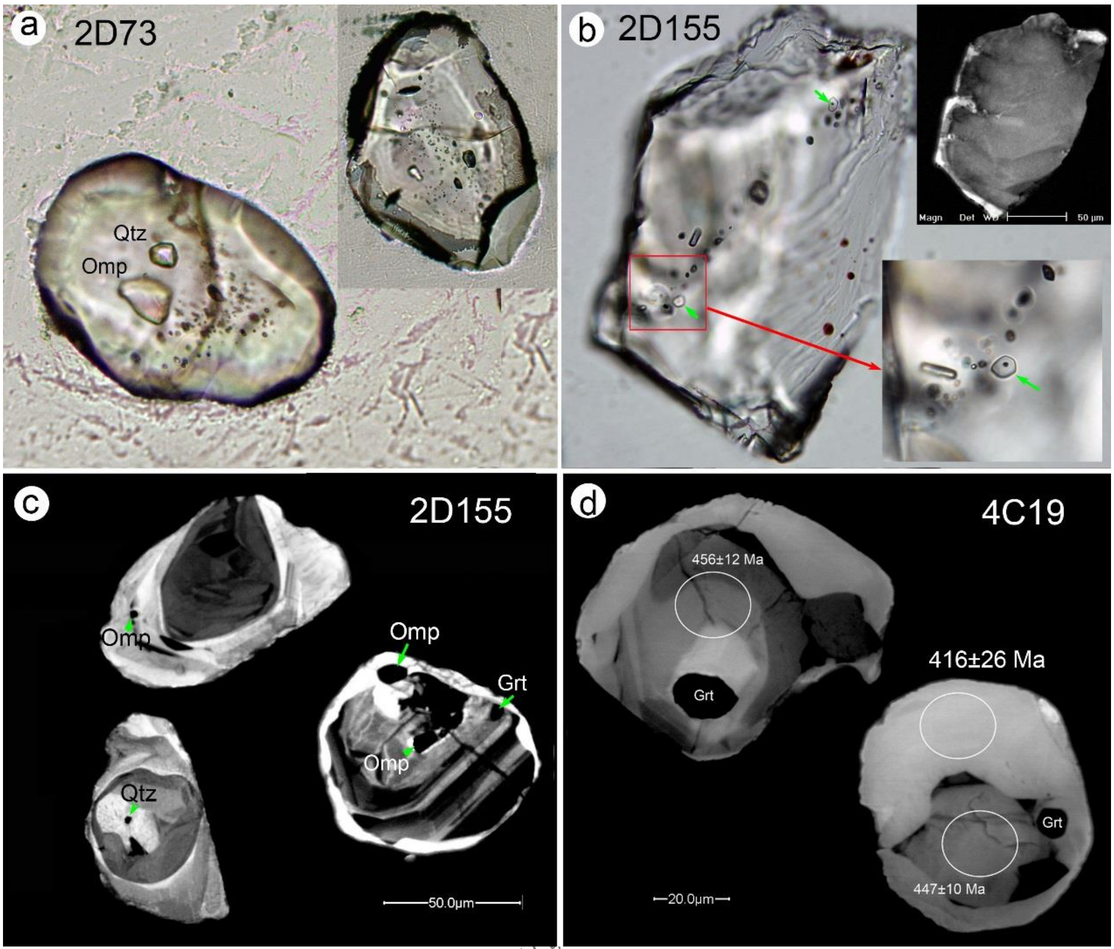

Fig. 4. Representative photomicrographs of zircons and their CL images. (a) Omp, quartz and small fluid inclusions in zircon cores (2D73). (b) A banded fluid inclusions in a zircon grain (2D155). These water-rich fluid inclusions show oval, tubular and negative-crystal shapes. The two negative-crystal inclusions (arrow) show major liquid phase with a small vapor bubble. (c) Zircon CL images showing obverse core-rim structure. The core domain contains Grt, Omp and Qtz inclusions, whereas the rim domain also has Omp inclusion. (d) Zircon CL images showing core-mantle structure with garnet inclusions and ages.

Evidence of two stages of metamorphic ages

Table 2 lists the published results of SHRIMP dating. Zircons from the basaltic eclogite 2D155 in the Yematan have large, dark-luminescence cores and narrow, intimidate-luminescence rims. Fourteen cores gave weighted $^{206}Pb/^{238}U$ mean age of 457± 7 Ma (MSWD = 0.91) and one rim gives an apparent age of 426±12 Ma (Song et al., 2006). For basaltic eclogite 2D73, two zircon grains contain relic magmatic cores and yielded $^{206}Pb/^{238}U$ apparent ages of 485 ± 24 Ma and 481 ± 24 Ma, which should represent the protolith age of the ophiolite sequence. Eight metamorphic cores analyzed by SHRIMP form a weighted $^{206}Pb/^{238}U$ mean of 462 ± 13 Ma (MSWD = 0.41) and fourteen analyses for rims and weak luminescent grains gave a weighted mean age of 424 ± 13 Ma (MSWD = 0.12). For basaltic eclogite sample 11YM 29, seventeen cores gave a weighted mean age of 448±6 Ma (MSWD = 0.91), and nine rims gave a weighted mean age of 425 Ma.

In the gabbroic sample (5S23) from the Shaliuhe UHP metamorphic ophiolite sequence, magmatic zircon relics with oscillatory zoning gave a weighted mean age of 517 ± 11 Ma (Zhang et al., 2008), suggesting the oceanic crust formed at late Cambrian, similar to ophiolite in the North Qilian suture zone (Song et al., 2013). Eleven metamorphic cores form a weighted mean age of 450 ± 7 Ma and thirteen rims and weak luminescent grains give a mean of 426 ± 13 Ma. Sample 4C05 is also a ky-eclogite from the Shaliuhe section. One zircon core gave a $^{206}Pb/^{238}U$ age of 468±16 Ma and 13 grains with intimidate-luminescence emission yielded weighted mean age of 425 ± 8 Ma.

Sample 4C19 is a garnet-pyroxenite metamorphosed from a high-Mg cumulate in Shaliuhe ophiolite sequence. Six analyses for dark-luminescence cores yield a weighted mean ages of 450 ± 7 Ma (MSWD = 0.31) and nine analyses for rims and weak luminescent grains gave a weighted mean age of 425 ± 9 Ma (MSWD =0.50).

Table 2. Zircon U-Pb SHRIMP ages of eclogites from Yematan ophiolitic section and Shaliuhe ophiolitic section.

sample	Rock type	Protolith age	stage I (core) (Lws-eclogite)	Stage II (rim) Ky/Zo-eclogite	Refs.

2D155	Basaltic eclogite (Yematan)	No magmatic core	457±7 Ma ***n*** = 15	426±12 Ma ***n*** = 1	Song et al. 2006; This study
2D73	Basaltic eclogite (Yematan)	485±23 Ma	452±15 Ma ***n*** = 10	424±13 Ma ***n*** = 14	Song et al., 2014a This study
11YM29	Basaltic eclogite (Yematan)	No magmatic core	448±6 Ma ***n*** = 17	425±6 Ma ***n*** = 9	Zhang et al. 2014
5S23	Gabbroic Ky-eclogite (Shaliuhe ophiolite)	517±11 Ma ***n*** = 10	450±7 Ma ***n*** = 11	426±13 Ma ***n*** = 13	Zhang et al. 2008
4C05	Gabbroic Ky-eclogite (Shaliuhe ophiolite)	No magmatic core	468±16 Ma ***n*** = 1	425±8 Ma ***n*** = 13	Song et al. 2014a
4C19	Grt-pyroxenite (Shaliuhe ophiolite)	No magmatic core	450 ± 11 Ma ***n*** = 6	425 ± 9 Ma ***n*** = 9	Song et al. 2014a

Evidence of zircon uranium contents and REE patterns

As a fluid-mobile element, uranium (U) is expected to enrich in zircon at a water-dominated fluid-rich environment. Figure 5 summarizes U contents of all zircons from the eclogite samples in Table 2. The magmatic relic zircon cores of the gabbroic Ky-eclogite have high and relatively uniform uranium content of 201-344 ppm (Fig. 5). The old metamorphic cores contain variable, but remarkably higher uranium content (40-800 ppm, mostly > 60 ppm) than the young metamorphic rims (7-141 ppm, mostly <50 ppm), suggesting that the core domain grew in a relatively wet, water-rich environment, whereas the rim domain grew in a relatively dry condition.

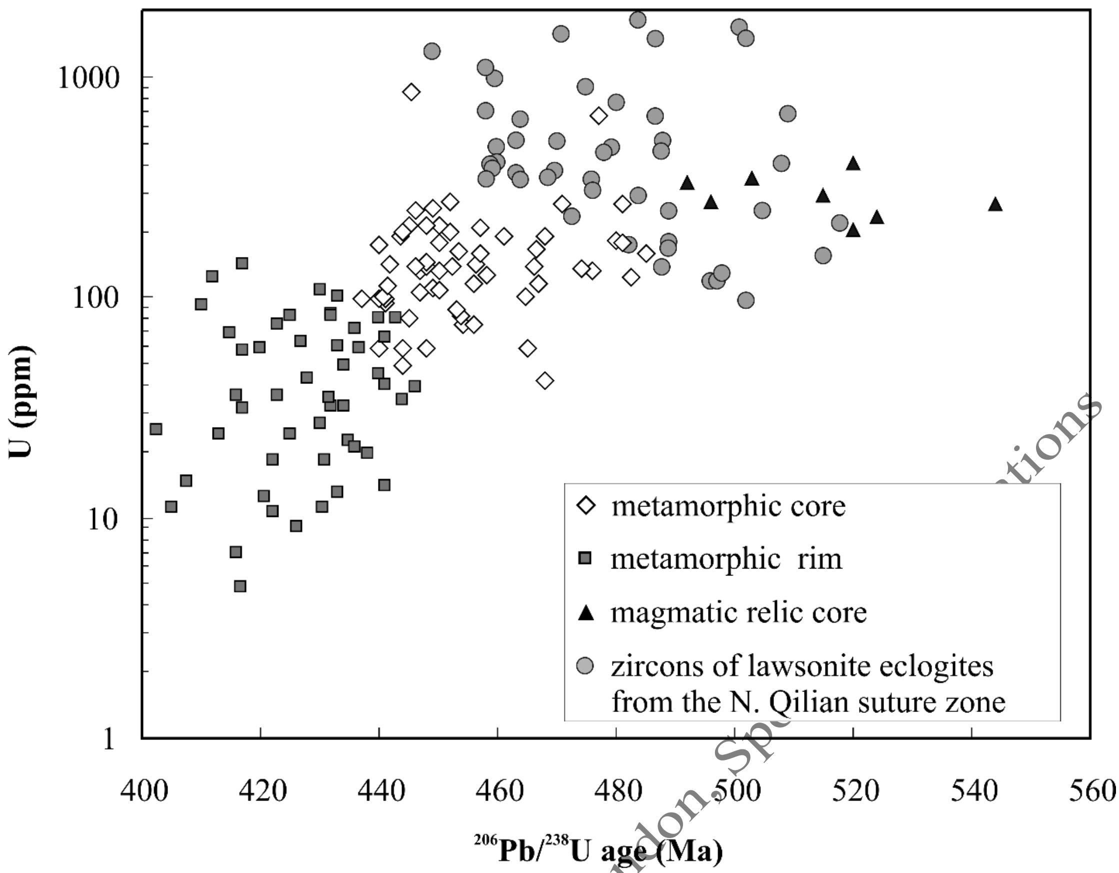

Fig. 5. Diagram for uranium vs. $^{206}Pb/^{238}U$ age of magmatic relics, metamorphic zircon cores and rims (samples are listed in Table 2). The magmatic relic cores are from the gabbroic eclogite sample (5S23, Zhang et al., 2008). Zircons of lawsonite-bearing eclogites are from the North Qilian suture zone (Song et al., 2004, 2006; Zhang et al., 2007)

Zircons from basaltic eclogite samples 2D73, 11YM29 and 2D155 were analyzed for trace elements, and zircon from one lawsonite eclogite sample (QS45) in the north Qilian suture zone are also analyzed for comparison (Fig. 6).

Zircons from the lawsonite eclogite (QS45) show dark luminescence with heterogeneous growth textures of "fir-tree" or radial sector zoning in the CL image (Fig 6a). Some zircon core parts are rich in HREE and show obvious negative Eu* anomaly (0.28-0.39), suggesting they might grow a little earlier than garnet, whereas the rim parts contains relatively lower HREE than the core parts and show no Eu* anomaly. All these zircons show steep HREE enriched pattern with high content of Yb and low

$[Tb/Yb]_N$ (0.05-0.24), which, together with their high U, suggesting that they grew together with lawsonite at a fluid-rich environment.

Three zircon inner-cores of sample 2D73 show similar REE patterns with, but have weaker Eu* anomaly (0.65-0.90) than, zircon cores of the Qilian lawsonite eclogite. Other cores show weakly enriched HREE patterns, and three zircons have extremely high light-REE, suggesting strong fluid activity. All rims (or whole grains with strong CL luminescent image) have low contents of REE and show flat or deplete HREE patterns with chondrite-normalized $[Tb]_N/[Yb]_N$ mostly > 1 (Fig. 6b).

Zircon cores of 11YM29 exhibit large variety of the REE patterns, changing gradually from steep heavy-REE pattern to flat heavy REE patterns (Fig. 6c). This variation is most probably in equilibrium with garnet from less to more garnet presence during zircon growth. All of them have no significant Eu anomaly, indicating the absence of coexisting plagioclase, and thus zircon growth at high pressure beyond the stability of feldspar (Rubatto et al., 2011). The zircon rims show depletion of HREE patterns with $[Tb]_N/[Yb]_N < 1$, suggesting that the supply of heavy-REEs decrease when growing.

Zircons from 2D155 have a large core with dark luminescence and fir-tree structure, and a thin bright rim. U-Pb analyses by the LA-ICP-MS gave a mean 206Pb/238U age of 459.5 ± 4 Ma (MSWD = 0.59), the same as by the SHRIMP dating (457 ±7 Ma). Trace element analyses show that zircons have rather uniform, weakly enriched HREE patterns ($[Tb]_N/[Yb]_N < 1$) and no Eu anomaly (Fig. 6d), similar to those metamorphic zircon cores described above.

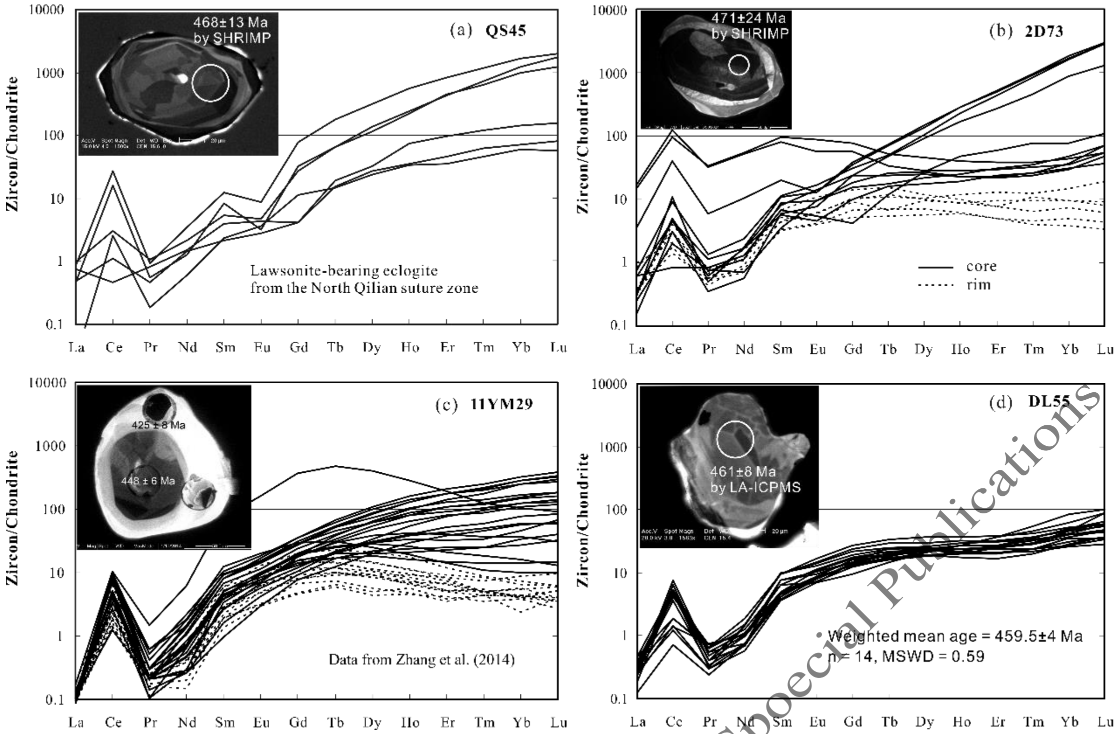

Fig. 6. Chondrite normalized REE patterns for zircons from (a) lawsonite eclogite (QS45) from the North Qilian Suture zone with a mean age of 464 ± 6 Ma (Song et al., 2006); (b) and (c) basaltic eclogite with two stages of zircon growth from the North Qaidam UHPM belt; (d) basaltic eclogite (2D155) with analyses of core-domains in the North Qaidam UHPM belt.

The steep heavy-REE pattern of zircon cores was generally thought that garnet, which readily sequesters heavy-REE, was not a major constituent of the assemblage, in other word, zircon would be grown earlier than garnet. However, garnet and omphacite inclusions in zircon cores suggest they must concurrently grew during eclogite-facies metamorphism. Therefore, we suggest that water-rich fluids will help heavy-REEs entering zircon against garnet, high Uranium contents in zircon cores can testify the explanation.

In summary, zircon U-Pb analyses show that two stages of HP-UHP metamorphism are distinct. The early HP stage from 448 Ma to 468 Ma with high uranium can be interpreted to be time for oceanic “wet and cold” subduction and the late stage from

430 Ma to 425 Ma for UHP metamorphism during continental subduction.

Discussion and conclusions

Two epochs of eclogite metamorphism at Oceanic vs. continental subduction

Seafloor subduction is generally cold (<550 °C, e.g. Maruyama et al., 1996; Carswell, 1990; Song et al., 2007; Agard et al., 2009) with abundant hydral minerals such as lawsonite, epidote/zoisite, glaucophene and carpholite (also see xiao et al., 2012, 2013). The minerals, especially lawsonite and carpholite, contain a large amount of water, and therefore can introduce the water into deep mantle along the oceanic subduction channels to depths greater than 100 km (e.g. Peacock and Wang, 1999; Poli and schemedt, 2002).

All studied eclogite samples came from ophiolitic sequences, the oceanic slab that previously preserved before continental collision. All lines of evidence described above, including (1) lawsonite pseudomorphs in garnet and their variation of composition profiles, (2) decrease of uranium contents from zircon core to rim, (3) REE patterns and two distinct stages of ages in metamorphic zircons, afford that they have experienced two cycles of eclogite-facies metamorphism. The first epoch is “cold and wet”, lawsonite-eclogite facies at P-T conditions of 2.6-2.7 GPa and 547-603°C related to the oceanic subduction, similar to, or little higher than, the lawsonite-eclogite in the North Qilian suture zone (e.g. Song et al., 2007; Zhang et al., 2007; Wei et al., 2009). The second epoch, on the other hand, is “dry and hot”, kyanite-eclogite facies at P-T conditions of 3.2-3.3 GPa and 700-720°C related to the continental subduction. The garnet peridotites, felsic gneisses and eclogites with protoliths of 850-820 Ma CFBs have experienced this epoch of UHP metamorphic event (see below).

Timescale of continental subduction

As described above, eclogites from the ophiolitic sequences have complex, but two distinct epochs of eclogite-facies metamorphic ages. However, some key rock types, including garnet peridotite, eclogites with CFB protolith and granitic and pelitic gneisses that represent the components of continental crust can be used to constrain the timescale of UHP metamorphism related to continental subduction.

(1) The garnet peridotite, which is only present in UHPM terranes associated with continental-type subduction zones (e.g., Brueckner, 1998), recorded UHP metamorphism at depths >200 km and gave UHP metamorphic ages of 433-420 Ma (Song et al., 2004, 2005ab; Xiong et al., 2011).

(2) Some eclogites in the North Qaidam UHMP belt have protoltihs of continental flood basalts (CFBs) with forming ages ranging 850 Ma to 820 Ma (e.g. Song et al., 2010). They are remarked components of the subducted continental crust. These eclogites recorded only a single UHP metamorphic event at ~ 438–425 Ma (Chen et al., 2009; Song et al., 2010; Zhang et al., 2010; Zhang et al., 2014).

(3) Zircons from pelitic and granitic gneisses in the North Qaidam recorded UHP metamorphic ages at 432-423 Ma (Mattinson et al., 2006, 2009; Song et al., 2006, 2014; Chen et al., 2009).

Therefore, These UHP metamorphic ages recorded by zircons indicate that continent crust subducted to depth 100 km might be at ~438 Ma and continued to depths 200 km at ~433-420 Ma. Assuming the Qilian Ocean was closed at ~445 Ma and the continents began to subduct with continental collision, the downgoing rate of the continental crust would be roughly 1.2-1.4 centimeters per year.

Melting of subducted oceanic slab evoked by continental subduction

Generally, the subducted continental crust is composed mostly of felsic gneisses (>80 %), buoyant and dry. The protoliths of eclogite are usually continental basalts (e.g. in the North Qaidam UHP belt, Song et al., 2010), cumulate gabbros or former high-grade metamorphosed granulite (e.g., Liu et al., 2007; Song et al., 2012) with extremely low-content of water, and they are difficult to melt during continental subduction and exhumation.

The former subducted oceanic slab is generally cold and wet with water-rich minerals, such as lawsonite, zoisite/epidote and glauscophane. The subsequent continental subduction can disturb the thermal structure of the subduction zone, and part of the subducting oceanic slab will roll back and be accreted to the subduction channel (e.g., Boutelier et al., 2004; Beaumont et al., 2009; Li et al., 2011; Gerya, 2011). Therefore, the former cold eclogites will be warmed up with dehydration reactions. When continental subduction initiated pulled by the its leading edge of subducting oceanic lithosphere, warmed up and then release water by dehydration of Lws and Ep, and give rise to partial melting by both decompression and water releasing (Song et al., 2014b). This process will in turn evoke exhumation of the UHP terrane (e.g., Labrousse et al., 2011).

Implications for linking oceanic subduction with continental subduction/collision

The onset of convergence can be constrained by youngest arc volcanic rocks, blueschist and low-T eclogites, and remnant sea-basin sediments. Arc volcanic rocks from the North Qilian and Lajishan, as well as low-T, high-pressure metamorphism at the Qilian oceanic suture zone, suggest that the Qilian Ocean was finally closed at ~ 445 Ma (Song et al., 2013), and continental subduction continuously followed the oceanic subduction and reach depths of 100-200 km at ~438-420 Ma on the basis of metamorphic and geochronological studies of eclogites, garnet peridotite and metapelite (Song et al., 2005, 2006, 2014a; Zhang et al., 2010; Xiong et al., 2011; Zhang et al., 2014). The timescale for transition from oceanic subduction to continental collision and then subduction to depths ~ 100 km is about 7 million years (Mys).

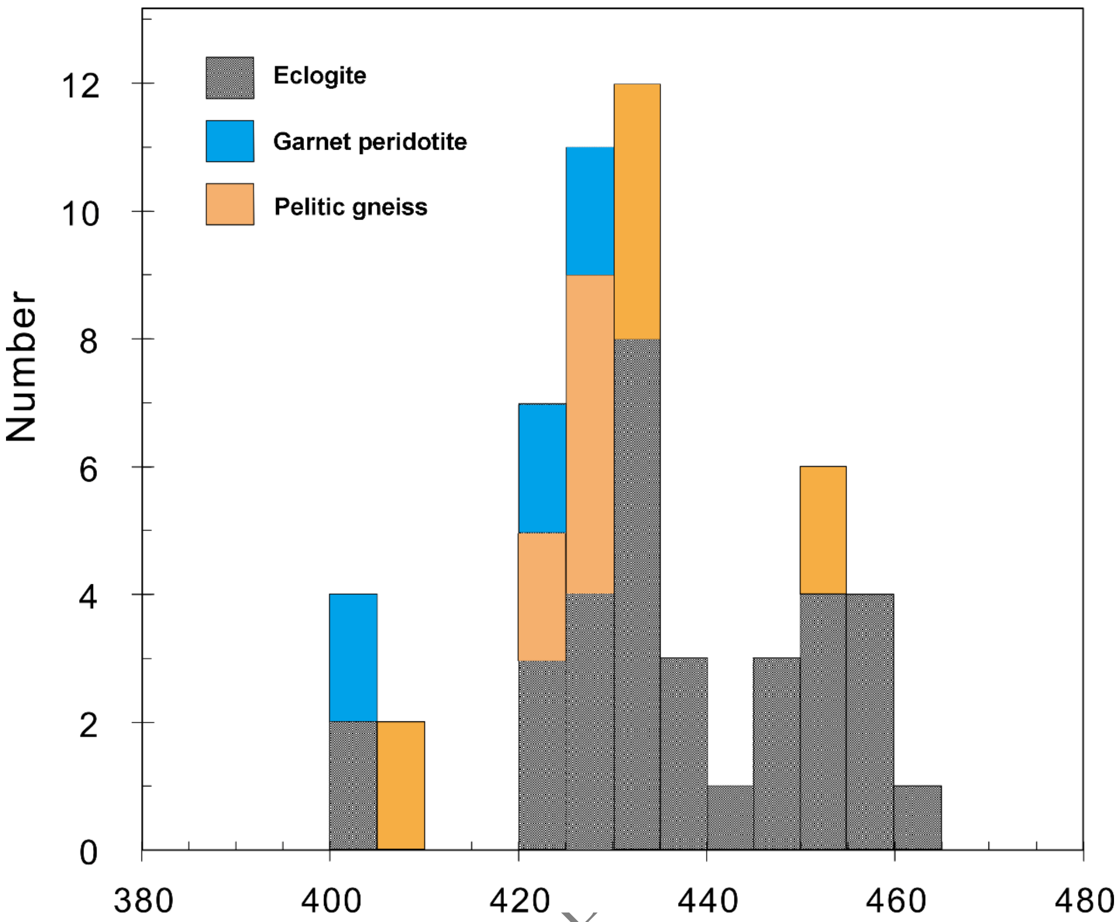

Fig. 7. Distribution of zircon U-Pb ages for various UHPM rocks from the North Qaidam UHPM belt. Data from Song et al. (2014, and references therein).

Distribution of all reliable zircon U-Pb ages for various UHPM rocks from the North Qaidam UHPM belt (Fig. 7) illustrates the two major epochs of metamorphism, except for the late (< 420 Ma) retrograde overprinting. The gap in between 440 Ma and 445 Ma with only one age presented, further suggested a transition from the end of oceanic subduction and continental colliding initiation at ~445 Ma, to continental deep subduction with UHP metamorphism at ~ 438-420 Ma.

Our study provide evidence for two epochs of eclogite-facies metamorphism in individual eclogite samples in the North Qaidam UHP belt, which recorded a complex, but a complete cycle from oceanic "cold" subduction to continental "warm" subduction in a timescale of ~40 Myr. Such a cycle may represent transition of subduction channel dynamics from Franciscan-type (or oceanic-type) (e.g. Gerya et al., 2002; Agard et al., 2009) to Alpine-type (or continental-type) (Ernst 2001; Song et al., 2006). In any case, the remarkable two epochs of eclogite-facies metamorphism present better understanding for links between the oceanic subduction and the followed continental collision and subduction.

Acknowledgments

This study was supported by the Major State Basic Research Development Program (2015CB856105), National Natural Science Foundation of China (Grant Nos.41372060, 41572040, 41121062, 41130314) and Basic geological survey program of China Geological Survey (1212011121258).

References

Agard, P., Yamato, P., Jolivet, L., and Burov, E. (2009). Exhumation of oceanic blueschists and eclogites in subduction zones: Timing and mechanisms. *Earth-Science Reviews* 92, 53-79.

Beaumont C., Jamieson R. A., Butler J. P. and Warren C. J. (2009) Crustal structure: a key constraint on the mechanism of ultrahigh-pressure rock exhumation. *Earth Planet. Sci. Lett.* 287,116–129.

Black, L. P., Kamo, S. L., Allen, C. M., Aleinikoff, J. N., Davis, D. W., Korsch, R. J. and Foudoulis, C. (2003). TEMORA 1: a new zircon standard for Phanerozoic U–Pb geochronology. *Chemical Geology* 200, 155–170.

Boutelier, D., Chemenda, A., Jorand C. (2004). Continental subduction and exhumation of high-pressure rocks: insights from thermo-mechanical laboratory modelling. *Earth Planet. Sci. Lett.* 222, pp. 209–216.

Brueckner H.K., Carswell D.A., and Griffin W.L. (2002). Paleozoic diamonds within a Precambrian peridotite lens in UHP gneisses of the Norwegian Caledonides. *Earth Planet. Sci. Lett.* 203, 805–816.

Brueckner, H.K. (1998). Sinking intrusion model from the emplacement of garnet-bearing peridotites into continent collision orogens. *Geology* 26, 631–634.

Brueckner, H.K. (2006). Dunk, dunkless and re-dunk tectonics: A model for metamorphism, lack of metamorphism, and repeated metamorphism of HP/UHP terranes. *Int. Geol. Rev.* 48, 978–995.

Brueckner, H.K. (2011). Geodynamics: Double-dunk tectonics. *Nature Geosci.* 4, 136-138.

Carswell, D. A. (1990). Eclogite Facies Rocks. Blackie (Glasgow & London), Chapman & Hall (New York), 396 pp.

Chemenda, A. I., Mattauer, M., and Bokun, A. N. (1996). Continental subduction and a mechanism for exhumation of high-pressure metamorphic rocks: new modelling and field data from Oman. *Earth Planet. Sci. Lett.* 143, 173–182.

Chen, D. L., Liu, L., Sun, Y., Liou, J. G. (2009). Geochemistry and zircon U–Pb dating and its implications of the Yukahe HP/UHP terrane, the North Qaidam, NW China. *Journal of Asian Earth Sciences* 35, 259-272.

Clarke, G. L., Aitchison, J. C. and Cluzel, D. (1997). Eclogites and blueschists of the Pam Peninsula, NE New Caledonia: a reappraisal. *Journal of Petrology* 38, 843–876.

Compston, W., Williams, I. S., Kirschvink, J. L., Zhang, Z. and Ma, G. (1992). Zircon U–Pb ages for the Early Cambrian time-scale. *Journal of the Geological Society, London* 149, 171–184.

Ernst, W.G. (2001). Subduction, ultrahigh-pressure metamorphism, and regurgitation of buoyant crustal slices—implications for arcs and continental growth. *Phys. Earth Planet. Inter.* 127, 253–275.

Ernst, W.G. (2005). Alpine and Pacific styles of Phanerozoic mountain building: subduction-zone petrogenesis of continental crust. *Terra Nova* 17, 165-188.

Gerya T. (2011). Future directions in subduction modeling. *J. Geodyn.* 52, 344–378.

Gerya, T., Stockhert, B. and Perchuk, A. (2002) Exhumation of high-pressure metamorphic rocks in a subduction channel: A numerical simulation. Tectonics 21, T1056.

Han L. (2015). Petrology study of Yematan eclogite from North Qaidam, China. Doctoral thesis of Peking University.

Herwartz, D., Nagel, T.J., Munker, C., Scherer, E.E. and Froitzheim, N. (2011). Tracing two orogenic cycles in one eclogite sample by Lu-Hf garnet chronometry. *Nature Geosci* 4, 178-183.

Labrousse L., Jolivet L., Andersen T. B., Agard P., Hebert R., Maluski H. and Scharer U. (2004) Pressure-temperature-time deformation history of the exhumation of ultra-high pressure rocks in the Western Gneiss Region, Norway. Geol. Soc. Am. Spec. Pap. 380, 155–183.

Li Z. H., Xu Z. Q. and Gerya T. V. (2011) Flat versus steep subduction: contrasting modes for the formation and exhumation of high- to ultrahigh-pressure rocks in continental collision zones. *Earth Planet. Sci. Lett.* 301, 65–77.

Liu, X.C., Wu, Y.B., Gao, S., Liu, Q., Wang, H., Qin, Z.W., Li, Q.L., Li, X.H. and Gong, H.J. (2012). First record and timing of UHP metamorphism from zircon in the Xitieshan terrane: Implications for the evolution of the entire North Qaidam metamorphic belt. *American Mineralogist* 97, 1083-1093.

Liu, Y. C., Li, S. G., Gu, X. F., Xu, S. T. and Chen, G. B. (2007). Ultrahigh-pressure eclogite transformed from mafic granulite in the Dabie orogen, east-central China. *J. Metamorph. Geol.* 25, 975-989.

Maruyama, S., Liou, J.G., and Terabayashi, M. (1996). Blueschists and eclogites of the world and their exhumation. *Int. Geol. Rev.* 38, 485–594.

Mattinson, C. G., Wooden, J. L., Liou, J. G., Bird, D. K. and Wu, C. L. (2006). Age and duration of eclogite-facies metamorphism, North Qaidam HP/UHP terrane, western China. *American Journal of Science* 306, 683-711.

Mattinson, C.G., Wooden, J.L., Zhang, J. and Bird, D.K. (2009). Paragneiss zircon geochronology and trace element geochemistry, North Qaidam HP/UHP terrane, western China. *J. Asian Earth Sci.* 35, 298–309.

Peacock, S. M. and Wang, K. (1999). Seismic consequences of warm versus cool subduction metamorphism: examples from southwest and northeast Japan. *Science* 286, 937–939.

Pearce, N.J.G., Perkins, W.T., Westgate, J.A., Gorton, M.P., Jackson, S.E., Neal, C.R. and Chenery, S.P. (1997). A compilation of new and published major and trace element data for

NIST SRM 610 and NIST SRM 612 glass reference materials. *Geostandards Newsletter* 21, 115–144.

Poli, S. and Schmidt, M. W. (2002). Petrology of subducted slabs. *Annu. Rev. Earth Planet. Sci.* 30, 207–35.

Ravna, E. J. K. and Terry, M. P. (2004). Geothermobarometry of UHP and HP eclogites and schists – an evaluation of equilibria among garnet–clinopyroxene–kyanite–phengite–coesite/quartz. *J. Metamorph. Geol.* 22, 579–592.

Rubatto, D., Regis, D., Hermann, J., Boston, K., Engi, M., Beltrando, M. and McAlpine, S. R. B. (2011). Yo-yo subduction recorded by accessory minerals in the Italian Western Alps. *Nature Geosci.* 4, 338-342.

Song, S. G., Niu, Y. L., Su, L. and Xia, X. H. (2013). Tectonics of the North Qilian orogen, NW China. *Gondwana Research* **23**, 1378-1401.

Song, S. G., Niu, Y. L., Su, L., Wei, C. J. & Zhang, L. F. (2014). Adakitic (tonalitic-trondhjemitic) magmas resulting from eclogite decompression and dehydration melting during exhumation in response to continental collision. *Geochimica et Cosmochimica Acta* 130, 42-62.

Song, S. G., Niu, Y. L., Su, L., Zhang, C. and Zhang, L. F. (2014a). Continental orogenesis from ocean subduction, continent collision/subduction, to orogen collapse, and orogen recycling: The example of the North Qaidam UHPM belt, NW China. *Earth-Science Reviews* 129, 59-84.

Song, S. G., Su, L., Niu, Y. L., Zhang, G. B. and Zhang, L. F. (2009). Two types of peridotite in North Qaidam UHPM belt and their tectonic implications for oceanic and continental subduction: A review. *J. Asian Earth Sci.* **35**, 285-297.

Song, S. G., Zhang, L. F., Niu, Y. L., Su, L., Song, B. and Liu, D. Y. (2006). Evolution from Oceanic Subduction to Continental Collision: a Case Study from the Northern Tibetan Plateau Based on Geochemical and Geochronological Data. *J. Petrol.* 47, 435-455.

Song, S. G., Zhang, L. F., Niu, Y. L., Wie, C. J., Liou, J. G. and Shu, G. M. (2007). Eclogite and carpholite-bearing metasedimentary rocks in the North Qilian suture zone, NW China: implications for early palaeozoic cold oceanic subduction and water transport into mantle. *J. Metamorph. Geol.* **25**, 547-563.

Song, S.G, Su, L., Li, X.-h., Zhang, G.B., Niu, Y.L. and Zhang, L.F. (2010). Tracing the 850-Ma continental flood basalts from a piece of subducted continental crust in the North Qaidam UHPM belt, NW China. *Precambrian Research* 183, 805-816.

Song, S.G., Su, L., Li, X.H., Niu, Y.L. and Zhang, L.F. (2012). Grenville-age orogenesis in the Qaidam-Qilian block: The link between South China and Tarim. *Precambrian Research* 220, 9-22.

Song, S.G., Yang, J.S., Liou J.G., Wu, C.L., Shi, R.D. and Xu Z.Q. (2003b). Petrology, Geochemistry and isotopic ages of eclogites in the Dulan UHPM terrane, the North Qaidam, NW China. *Lithos* 70 (3-4), 195-211.

Song, S.G., Yang, J.S., Xu, Z.Q., Liou, J.G., Wu, C.L. and Shi, R.D. (2003a). Metamorphic evolution of coesite-bearing UHP terrane in the North Qaidam, northern Tibet, NW China. *J. Metamorph. Geol.* 21, 631-644.

Song, S.G., Zhang, L.F., Niu, Y. (2004). Ultra-deep origin of garnet peridotite from the North Qaidam ultrahigh-pressure belt, Northern Tibetan Plateau, NW China. *American Mineralogist* 89, 1330–1336.

Song, S.G., Zhang, L.F., Niu, Y.L., Su, L., Jian, P. and Liu, D.Y. (2005). Geochronology of diamond-bearing zircons from garnet peridotite in the North Qaidam UHPM belt, Northern Tibetan Plateau: A record of complex histories from oceanic lithosphere subduction to continental collision. *Earth Planet. Sci. Lett.* 234, 99-118.

Stacey, J. S. and Kramers, J. D. (1975). Approximation of terrestrial lead isotope evolution by a two-stage model. *Earth Planet. Sci. Lett.* 26, 207–221.

Tsujimori, T., Ernst, W.G., 2014. Lawsonite blueschists and lawsonite eclogites as proxies for palaeo-subduction zone processes: a review. Journal of Metamorphic Geology 32, 437-454.

Wei, C.J., Yang, Y., Su, X.L., Song, S.G. (2009). Metamorphic evolution of low-T eclogite from the North Qilian orogen, NW China: evidence from petrology and calculated phase equilibria in the system NCKFMASHO. *J. Metamorph. Geol.* 27, 55–70.

Whitney, D.L. and Evans, B.W. (2010). Abbreviations for names of rock-forming minerals. *American Mineralogist* 95, 185–187.

Xiong, Q., Zheng, J., Griffin, W.L., O'Reilly, S.Y. and Zhao, J. (2011). Zircons in the Shenglikou ultrahigh-pressure garnet peridotite massif and its country rocks from the North Qaidam terrane (western China): Meso-Neoproterozoic crust–mantle coupling and early Paleozoic convergent plate-margin processes. *Precambrian Res.* 187, 33–57.

Yang, J.S., Xu, Z.Q., Song, S.G., Zhang, J.X., Wu, C.L., Shi, R.D., Li, H.B., Brunel, M. and Tapponnier, P. (2002). Subduction of continental crust in the early palaeozoic North Qaidam ultrahigh-pressure metamorphic belt, NW China: Evidence from the discovery of coesite in the belt. Acta Geologica Sinica-English Edition 76, 63-68.

Zhang, G.B., Song, S. G., Zhang, L. F. and Niu, Y. L. (2008). The subducted oceanic crust within continental-type UHP metamorphic belt in the North Qaidam, NW China: Evidence from petrology, geochemistry and geochronology. *Lithos* 104, 99-118.

Zhang, G.B., Zhang, L. F., Christy, A. G., Song, S. G. and Li, Q. L. (2014). Differential exhumation and cooling history of North Qaidam UHP metamorphic rocks, NW China: Constraints from zircon and rutile thermometry and U-Pb geochronology. *Lithos* **205**, 15-27.

Zhang, G.B., Zhang, L.F., Song, S.G., (2009a). UHP metamorphic evolution and SHRIMP geochronology of a metaophiolitic gabbro in the North Qaidam, NW China. Journal of Asian Earth Sciences 35, 310–322.

Zhang, J.X. Mattinson C.G., Yu S.Y., Li J.P. and Meng, F.C. (2010). U–Pb zircon geochronology of coesite-bearing eclogites from the southern Dulan area of the North Qaidam UHP terrane, northwestern China: spatially and temporally extensive UHP metamorphism during continental subduction. *J. metamorph. Geol.* 28, 955–978.

Zhang, J.X., Meng, F.C. and Wan, Y.S. (2007). A cold Early Palaeozoic subduction zone in the North Qilian Mountains, NW China: petrological and U–Pb geochronological constraints. *J. Metamorph. Geol.* 25, 285–304.